European Journal of Immunology

Supporting Information

for

DOI 10.1002/eji.201344219

Anca Dorhoi, Vladimir Yeremeev, Geraldine Nouailles, January Weiner 3rd, Sabine Jörg, Ellen Heinemann, Dagmar Oberbeck-Müller, Julia K. Knaul, Alexis Vogelzang, Stephen T. Reece, Karin Hahnke, Hans-Joachim Mollenkopf, Volker Brinkmann and Stefan H. E. Kaufmann

Type I IFN signaling triggers immunopathology in tuberculosis-susceptible mice by modulating lung phagocyte dynamics

© 2014 The Authors. *European Journal of Immunology* published by WILEY-VCH Verlag GmbH & Co. KGaA, Weinheim

Type I IFN signaling triggers immunopathology in tuberculosis-susceptible mice by modulating lung phagocyte dynamics

Anca Dorhoi[1,*], Vladimir Yeremeev[1,2,*],Geraldine Nouailles[1], January Weiner 3rd [1], Sabine Jörg[1], Ellen Heinemann[1], Dagmar Oberbeck-Müller[1], Julia Knaul[1], Alexis Vogelzang[1], Stephen T. Reece[1], Karin Hanke[1], Hans-Joachim Mollenkopf[1,3], Volker Brinkmann[4], Stefan H.E. Kaufmann[1]

Supporting Information: Figures 1–7

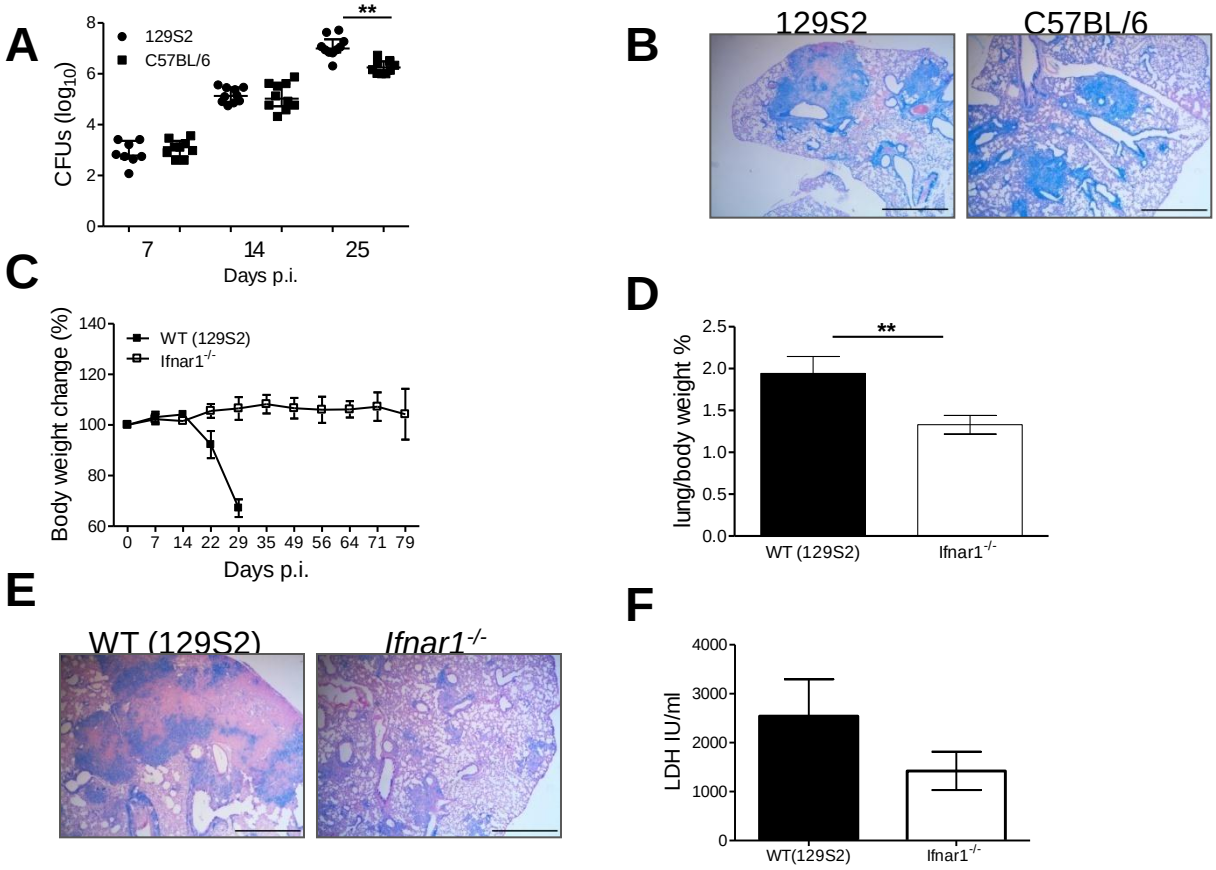

Supporting Information: Figure 1

Characteristics of TB disease in susceptible and resistant mice and in *Ifnar1*$^{-/-}$ animals. (A) Bacterial burdens in lungs of *Mycobacterium tuberculosis* (Mtb)-infected 129S2 and C57BL/6 mice (~200 CFUs; n_{pooled}=8-10; median±IQR). Data from two independent experiments, Mann-Whitney test for statistical analysis. (B) Histopathology of lungs, Giemsa staining of paraffin-embedded tissue collected at 25 days p.i. (scale bar, 1000 µm; n=5). Data from one representative of three independent experiments. (C) Relative body weights of WT (129S2) and *Ifnar1*$^{-/-}$ mice infected with low-dose of Mtb (~200 CFUs) (n_{pooled}=8-10; mean±SEM). Data from two experiments**.** (D) Relative lung weights of WT (129S2) and *Ifnar1*$^{-/-}$ mice at day 21 p.i. (n_{pooled}=8-9; mean±SEM). Data from two independent experiments. (E) Lung pathology, Giemsa staining of paraffin-embedded tissue collected at 25 days p.i. (scale bar, 1000 µm; n=5). Data from one representative of two independent experiments. (F) Serum concentrations of lactate dehydrogenase at day 21 p.i. in WT mice (129S2) and *Ifnar1*$^{-/-}$ mice (background 129S2) (n_{pooled} =11-13; mean±SEM). Data from two independent experiments. ** P < 0.01

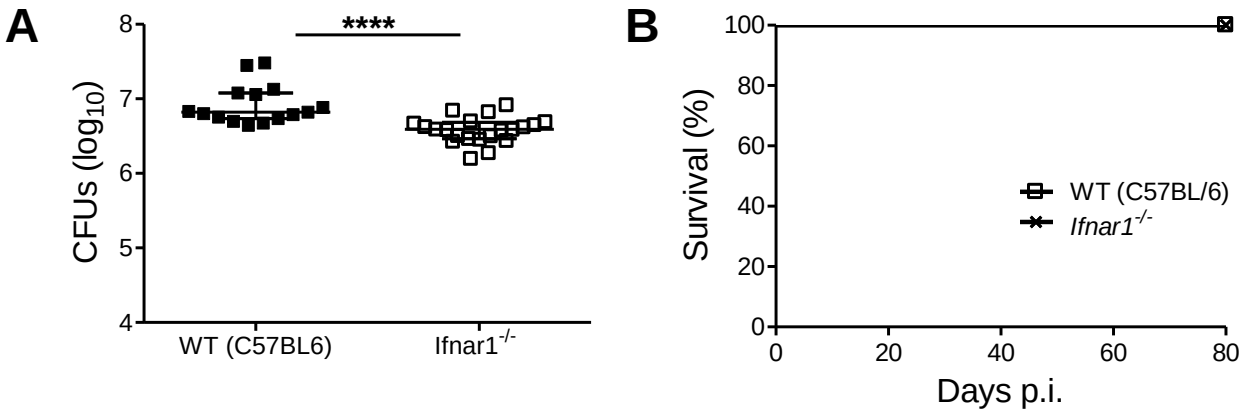

Supporting Information: Figure 2

TB disease in C57BL/6 and corresponding *Ifnar1*$^{-/-}$ animals. (A) Bacterial burdens (day 42) in lungs of infected WT (C57BL/6) and *Ifnar1*$^{-/-}$ mice (~500 CFUs; n_{pooled} =15–21; median±IQR). Data from two independent experiments, Mann–Whitney test for statistical analysis. (B) Survival of WT (C57BL/6), and *Ifnar1*$^{-/-}$ mice (n_{pooled} =12–20) after aerosol infection with virulent Mtb H37Rv (~200 CFUs), Kaplan–Meier curves. Data from two independent experiments. **** $P < 0.0001$

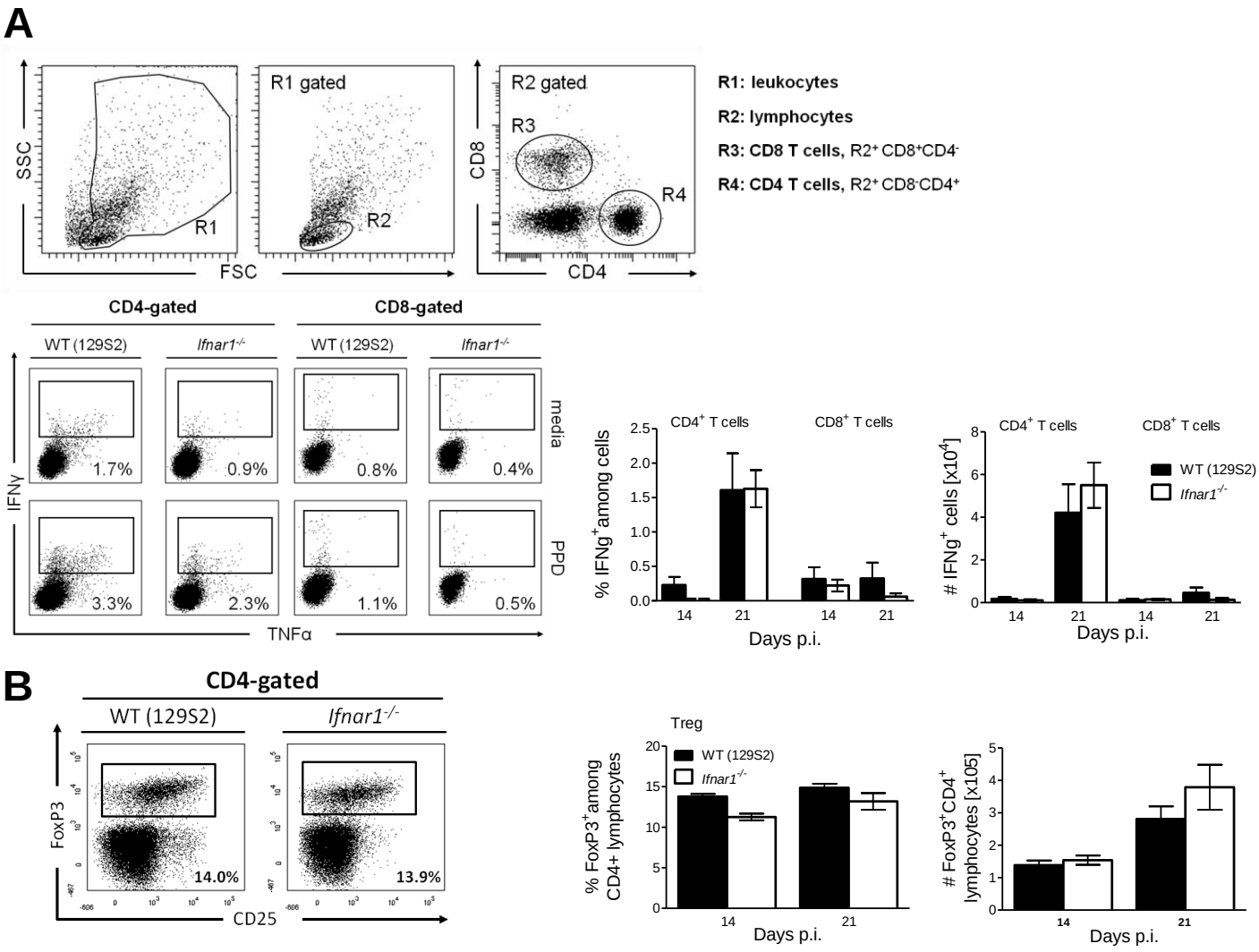

Supporting Information: Figure 3

Type I IFN signaling does not modify T cell responses. WT (129S2) and *Ifnar1*$^{-/-}$ mice were infected with Mtb and leukocyte populations isolated from lungs and analyzed by flow cytometry at indicated time points. (A) Flow cytometric gating strategy used for analysis of T cells. Frequencies of IFN-γ$^+$ cells among lung CD4$^+$ and CD8$^+$ T cells and numbers of IFN-γ$^+$TNF-α$^+$ lung CD4$^+$ and CD8$^+$ T cells after short-term *in vitro* restimulation with Mtb-derived PPD (n_{pooled}=8–10; mean±SEM). (B) Frequencies of FoxP3$^+$ cells among lung CD4$^+$ T cells and numbers of FoxP3$^+$CD4$^+$ lung lymphocytes (n_{pooled}=8–10; mean±SEM). (A–B) Mean values from two independent experiments.

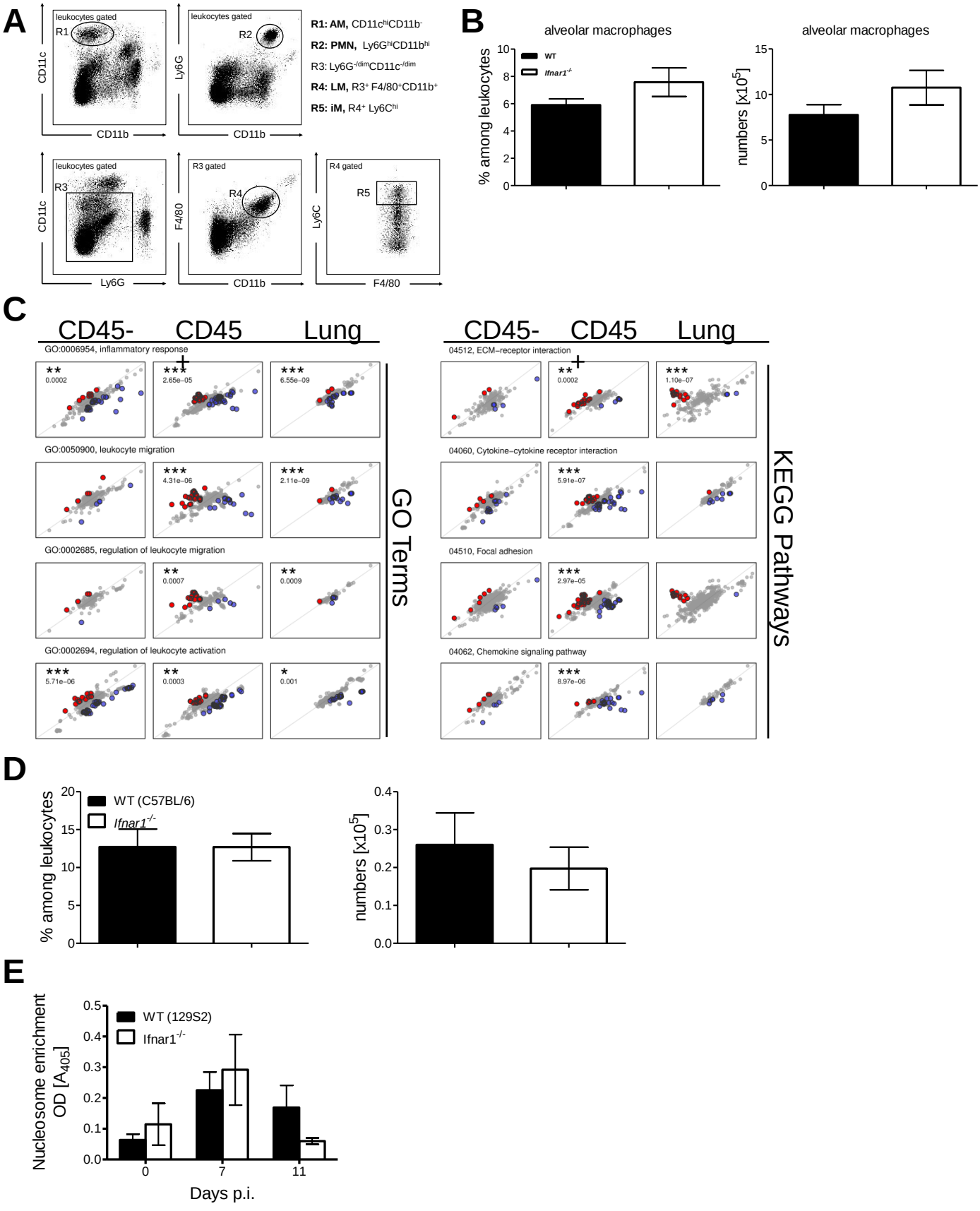
A
leukocytes gated
R1
CD11c
CD11b
leukocytes gated
R2
Ly6G
CD11b
R1: AM, CD11c^hiCD11b^-
R2: PMN, Ly6G^hiCD11b^hi
R3: Ly6G^-/dimCD11c^-/dim
R4: LM, R3^+ F4/80^+CD11b^+
R5: iM, R4^+ Ly6C^hi
leukocytes gated
R3
CD11c
Ly6G
R3 gated
R4
F4/80
CD11b
R4 gated
R5
Ly6C
F4/80
B
alveolar macrophages
% among leukocytes
WT
Ifnar1-/-
alveolar macrophages
numbers [x10^5]
C
CD45-
CD45
Lung
GO:0006954, inflammatory response
GO:0050900, leukocyte migration
GO:0002685, regulation of leukocyte migration
GO:0002694, regulation of leukocyte activation
GO Terms
04512, ECM–receptor interaction
04060, Cytokine–cytokine receptor interaction
04510, Focal adhesion
04062, Chemokine signaling pathway
KEGG Pathways
D
% among leukocytes
WT (C57BL/6)
Ifnar1-/-
numbers [x10^5]
E
Nucleosome enrichment
OD [A405]
WT (129S2)
Ifnar1-/-
Days p.i.

Supporting Information: Figure 4

Analysis of lung cell populations in WT and *Ifnar1*$^{-/-}$ mice during TB. (A) Flow cytometric gating strategy used for analysis of lung-innate cells: AMs (CD11c^{hi}CD11b^{-}), PMNs (Ly6G^{hi}CD11b^{hi}), LMs (CD11c^{-}Ly6G^{-} F4/80^{+}CD11b^{+}), iMs (CD11c^{-}Ly6G^{-} F4/80^{+}CD11b^{+} Ly6C^{hi}). (B) Numbers and frequencies of AMs in naive WT (129S2) and *Ifnar1*$^{-/-}$ mice (n=10; mean±SEM). Data representative of two experiments. (C) GO enrichment and KEGG pathway analysis. Left: Plots show log fold changes in gene expression between naive mice and day 14 p.i. for the WT (129S2) strain (horizontal axis) and the IFNAR1 KO (vertical axis) strain; each point corresponds to one gene from the given GO category. Three-plot columns correspond to the samples tested: CD45^{-} cells, CD45^{+} cells and RNA isolated from the whole lung. Genes depicted in color show significant interactions between infection and mouse strain. **Red** denotes genes for which log fold change is higher in the KO than in WT, and **blue** marks genes for which log fold change is higher in the WT than in KO. P-values correspond to significance of GO enrichment. Right: SPIA analysis of KEGG pathways. P-values correspond to the pGFWER composite p-value from the SPIA analysis. (D) PMN frequencies and numbers in BAL obtained at 14 days p.i. from C57BL/6 and corresponding *Ifnar1*$^{-/-}$ mice infected with virulent Mtb H37Rv (500 CFUs). Results are from one experiment (n=5; mean±SEM). (E) Nucleosome abundance in BALF obtained from naïve animals or at 7 and 10 days p.i. Data from two independent experiments (n_{pooled}=11; mean±SEM).

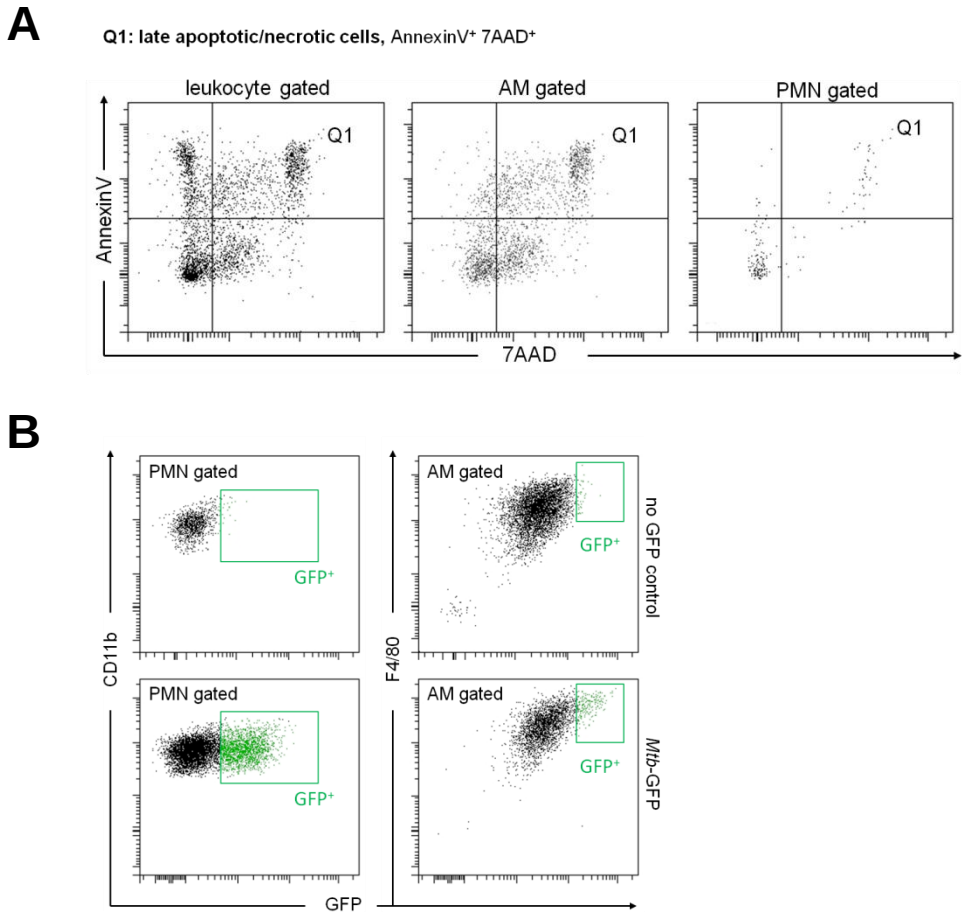

Supporting Information: Figure 5

Analysis of cell death and bacterial content within myeloid BAL cells during TB. Flow cytometric gating strategy used for (A) analysis of cell death events within BAL cells and (B) identification of Mtb-GFP cells within airways. Cells were gated using surface makers depicted in Fig. S4A to identify AMs and PMNs and subsequently dead cells were identified as annexinv^{+}7AAD^{+} (A) or the GFP signal was identified using samples from naïve mice or mice infected with wild-type Mtb, lacking the GFP reporter (B).

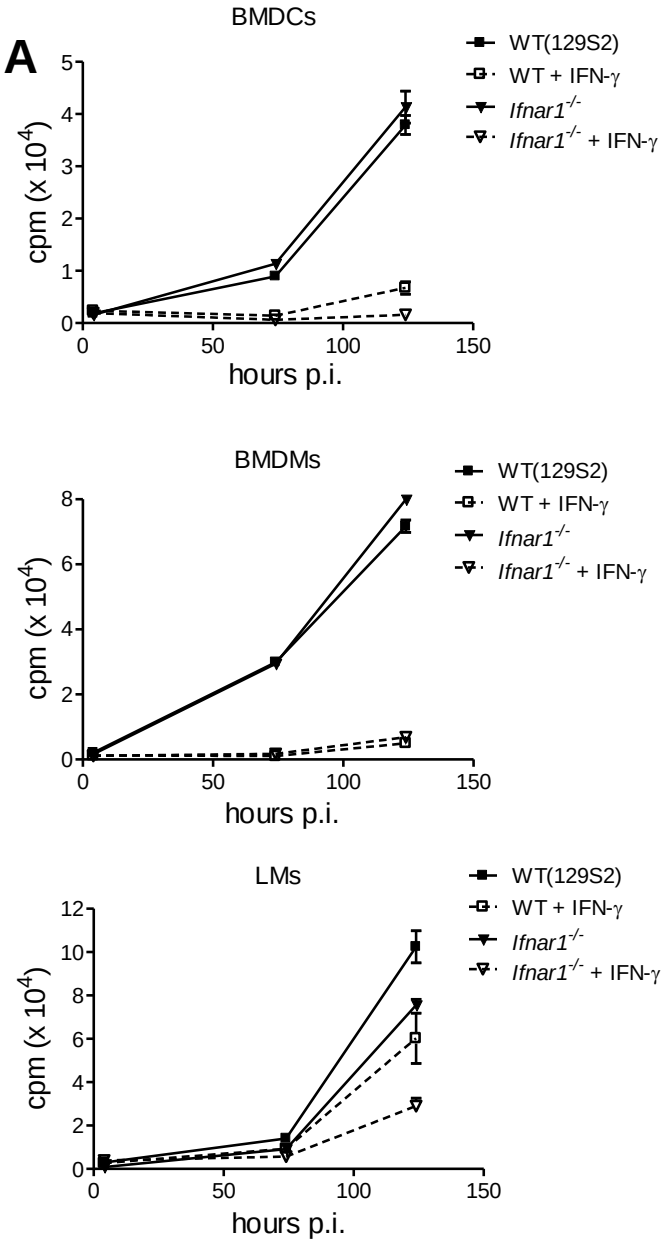

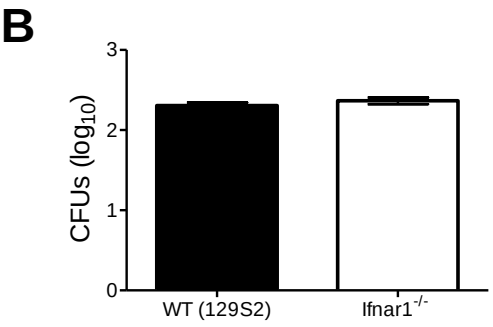

Supporting Information: Figure 6

Mtb phagocytosis and replication in BM-derived phagocytes, lung macrophages and alveolar macrophages . (A) BMDMs, BMDCs and LMs were infected with Mtb at MOI 5 and bacterial replication was determined by [3H]uracil uptake at different time points p.i. Data from one representative of three independent experiments with three replicates each. (B) AMs were infected with Mtb at MOI 10 and bacterial uptake was estimated by CFUs at 4 hours p.i. Data from one representative of two independent experiments with three to four replicates each.

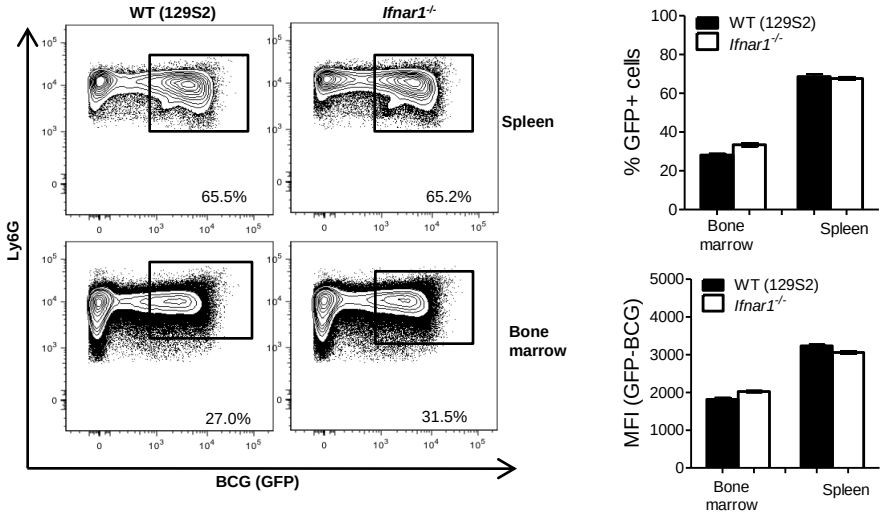

Supporting Information: Figure 7

Phagocytic properties of WT (129S2) and *Ifnar1*$^{-/-}$ cells for mycobacteria. Representative FACS plots showing phagocytosis of GFP-BCG by Ly6G^{+} PMNs purified from BM and spleen from WT (129S2) and *Ifnar1*$^{-/-}$ mice, two independent experiments with two to three replicates each.